Zhongguo Kuangye Daxue Xuebao
Journal of China University of Mining and Technology

2024 | Vol 29 | Issue 3 | Page 17-31
Journal Homepage: https://zkdx.ch/
DOI: 10.1654/zkdx.2024.29.3-2

Analysis of Large Diameter Bored Monopile under Static Axial Load

Baset M. A.
Ph.D Student, Geotechnical Eng. Division, Al-Azhar University, Cairo, Egypt

Bahr M. A.
Professor of Geotechnical Eng., Al-Azhar University, Cairo, Egypt

Hassan A. A.
Assistant Professor of Geotechnical Eng., Al-Azhar University, Cairo, Egypt

El-Attar A. N.*
Lecturer of Geotechnical Eng., Higher technology institute, Tenth of Ramadan City, Egypt
*Corresponding author

Abstract
Large-diameter monopiles with a diameter exceeding 0.60 m provide optimized foundation solutions for rather heavy structures. Egyptian code practice applies the basic design equations or field data from SPT-N to calculate pile capacity. A case study of a full-scale in-situ pile loading test at the Cairo Monorail project has been carried out and the pile was constructed in dense sand soil. The present study focuses on modeling a field vertical loading test performed on a large 2.0m diameter pile using Plaxis 3D. A modified finite model is proposed in this study for the analysis of pile axial load capacity to investigate the soil-pile behavior in terms of skin friction and end bearing. The vertical load versus settlement curve for the single pile field test is compared with that obtained from the finite element model, showing fair agreement. Parametric studies have been conducted to investigate the optimum length of the pile and its effect on pile capacity. Accordingly, some correlations and appropriate constitutive relationships for an ultimate vertical load of bored large-diameter piles embedded in sandy soil are reported by changing the length (Li) of the pile. Also, the comparison between Chin and ECP methods is presented for estimating the ultimate capacity of the pile. The results show that the accuracy of Chin method is depended on the pile length and testing pile load also, the ultimate capacity of pile demonstrated from Chin method is overestimated by comparing its result by that calculated from ECP method.

Keywords
Monopiles, Large Diameter Pile, Pile Bearing Capacity

1. Introduction
Large-diameter bored monopiles are used for heavy loads or the serviceability requirements of projects. Also, monopiles are used in the case of not enough area to construct piles group. The practical design of large diameter piles depended on the correlation based on SPT and soil investigation to determine both unit shaft resistance and unit tip resistance of the pile. Besides, full-scale loading tests are widely accepted as the best method for determining the bearing behavior of bored piles [3]. However, the cost of pile load test is expensive. Accordingly, the numerical analysis of the behavior of large-diameter piles is an appropriate solution to simulate the procedure of execution and loading of piles in the field.
There are several studies related to large-diameter bored pile behavior [1]. Modeled ten pile behaviors using Plaxis 3D and Chin method to evaluate pile ultimate capacity for the piles. These piles were not reached to failure load. The length of piles is 24 m and the range of pile diameters is from 0.6 to 0.8 m. In situ tests data were compared by that calculated from numerical simulation. The results indicate that there is excellent agreement between field and numerical result which indicates the capability of finite element. Also, the results have demonstrated that the pile capacity estimated from the simulation process is larger by about 51% than that estimated before the design of piles [8] established a finite element model to simulate the behavior of a large diameter bored pile, installed in multi-layered soil at Damietta Port. The axial loads are up to 9.0 MN where pile settlements are 22.8 and 23.3 mm in the field and numerical model respectively.

The results demonstrated that about 83% of the applied load was transferred by friction and about 17% of the total load was carried by bearing while the settlement at failure load is 5.5% pile diameter. In addition, the results showed

that the plastic zone below the base of the pile at failure extended laterally to about seven times the pile diameter and vertically to about 5 times the pile diameter [9] presented a numerical model to simulate a large-diameter pile under axial force by implementing different soil models. This numerical model is conducted on pile diameter and length of 1.30 m and 9.50 m respectively. The results showed that the MMC constitutive model is outstanding compared to MC and SS models in predicting the ultimate base and shaft resistances of the large diameter bored pile. Also, the comparison between field measurements and finite element results of pile bearing, friction, total load, and settlement were presented. They documented that the skin friction achieved its peak value at a settlement value equal to 1.5% D. [2] compared two full-scale pile load test results with numerical modeling using both Plaxis 2D and Plaxis 3D software. The diameter of piles is 1.0 m, the pile lengths are 29.2, 46.0 m. The results observed with pile models in Plaxis 3D are comparably better as of the axisymmetric model [12] presented numerical modeling of end-bearing piles constructed in thick layers of soft to very soft clay underlain by a dense sand layer. The pile diameter and length are 1.2 m and 70.0 m respectively. The effect of pile diameter on pile capacity was studied depending on settlement-diameter ratios. Moreover, they found that the failure load practically took place at settlement ranging from 4.0%D to 5.0%D.

The paper initially discusses the outcomes of an extensive vertical pile loading test. Subsequently, a numerical model is developed to mirror the data gathered from the field test, with the aim of verifying the model's ability to simulate the process of the pile loading test. This model is then used to calculate and determine the maximum capacity of the pile tested.

The second part of the study involves a parametric analysis using finite element methods to alter the length of the pile. Subsequently, the bearing behavior is estimated by calculating the axial load and observing soil deformation. This leads to the determination of both the unit shaft resistance and the unit tip resistance of the pile.

In the final section, the data obtained from the loading test and the Finite Element Method (FEM) analysis is compared with theoretical design calculations. Based on these comparisons, the paper proposes some considerations for a design method aimed at estimating the bearing capacity of large diameter bored piles. Finally, the relationship between stress and displacement is analyzed to estimate pile settlement and the ultimate capacity.

1.1 Estimation of Ultimate Load

Generally, the ultimate load is determined when the settlement increases at constant loading which is not demonstrated during the pile test. Theoretically, the ultimate load value is specified at settlement equal to 10% of the pile diameter according to the Euro code 7 of geotechnical design [4]. However, the ultimate load is not outlined at 10% pile diameter (200 mm). Consequently, such a definition of ultimate load requires increasing the test load up to the failure state as shown in the next section. In addition, the ultimate capacity of pile is calculated using theoretical equation based on shaft resistance and the tip resistance;

$$\boldsymbol{Q_u = Q_{bu} + Q_{su}} \quad \textbf{(1)}$$

where Q_{bu} and Q_{su} are the ultimate capacity of end bearing and skin friction respectively. The end bearing capacity at applied load is determined by the equation;

$$\boldsymbol{Q_b = q_b \,.\, A_p} \quad \textbf{(2)}$$

where q_b is the bearing resistance and A_p is the area of pile tip. The shaft load of pile is calculated by summation of the shear forces along the pile length.

$$\boldsymbol{Q_s = \sum P\,(dL)\,q_s} \quad \textbf{(3)}$$

where P is the pile perimeter at any section dL, and q_s is unit shaft resistance.

1.2 Practical Estimation of Ultimate Load of Large Diameter Bored Piles According to ECP.

Large diameter piles definition is that piles with diameter larger than 60 cm [3]. The design of large diameter piles according to Egyptian code is depended on OKCJ chart. **Fig. 1** shows OKCJ line which is the summation of two lines, OBH and OAG lines of pile unit tip resistance and shaft resistance respectively.

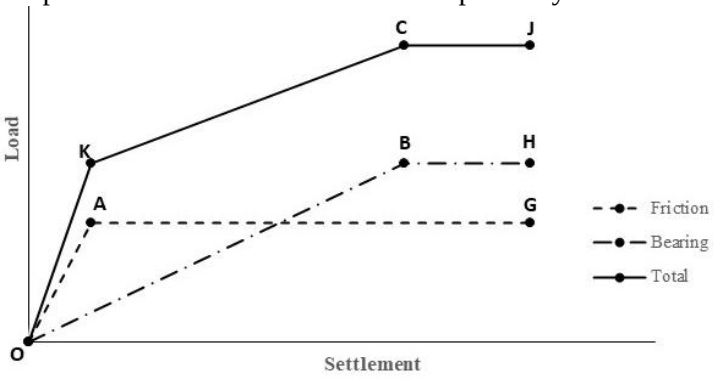

Fig. 1 OKCJ chart (ECP 202-2001)

For cohesionless soils, point A is the intersection of pile settlement equal to 1% of the pile diameter with the friction load along the pile that is determined according to Table 1.

Table 1 Shaft resistance for large diameter bored piles in sand (ECP 202-2001)

SPT-N	Depth from ground level (m)	Shaft resistance (kN/m^2)
Less than 10	-	0.00
From 10 to 20	0.00 – 2.00	0.00
	2.00 – 5.00	30.00
	> 5.00	50.00
From 20 to 30	0.00 – 2.00	0.00
	2.00 – 7.50	45.00
	> 7.50	75.00
Greater than 30	0.00 – 2.00	0.00
	2.00 – 10.00	60.00
	> 10.00	100.00

Also, point B is the intersect of pile settlement equal to 15 cm with the pile tip load that determined according to Table 2.

Table 2 Unit tip resistance for large diameter bored piles in sand (ECP 202-2001)

Settlement	Unit tip resistance (MN/m^2)	
(cm)	**Belled end**	**Straight end**
1.00	0.35	0.50
2.00	0.65	0.80
3.00	0.90	1.10
15.00*	2.40	3.40

**Settlement at ultimate load*

2. Vertical Loading Test on Bored Piles

Full-scale static compression pile load test was considered as case study from Cairo Monorail project constructed in 6th of October line. This loading test was conducted in June 2021. Table 3 shows the description of the pile and loading test.

Table 3 Description of loading test on bored pile (Consulting Bureau Prof. Adel Gabr, 2020)

Pile No.	01
Pile Diameter, D (m)	2.00
Pile length, L (m)	18.00
Pile design load (Q_d) (ton)	500
Test load (P_o) (ton)	1250

Generally, the piles used in the Monorail are monopiles, and the monopile carries one circular column without a footing. The monopile and the column are connected directly by the reinforcing as one member as shown in Fig. 2.

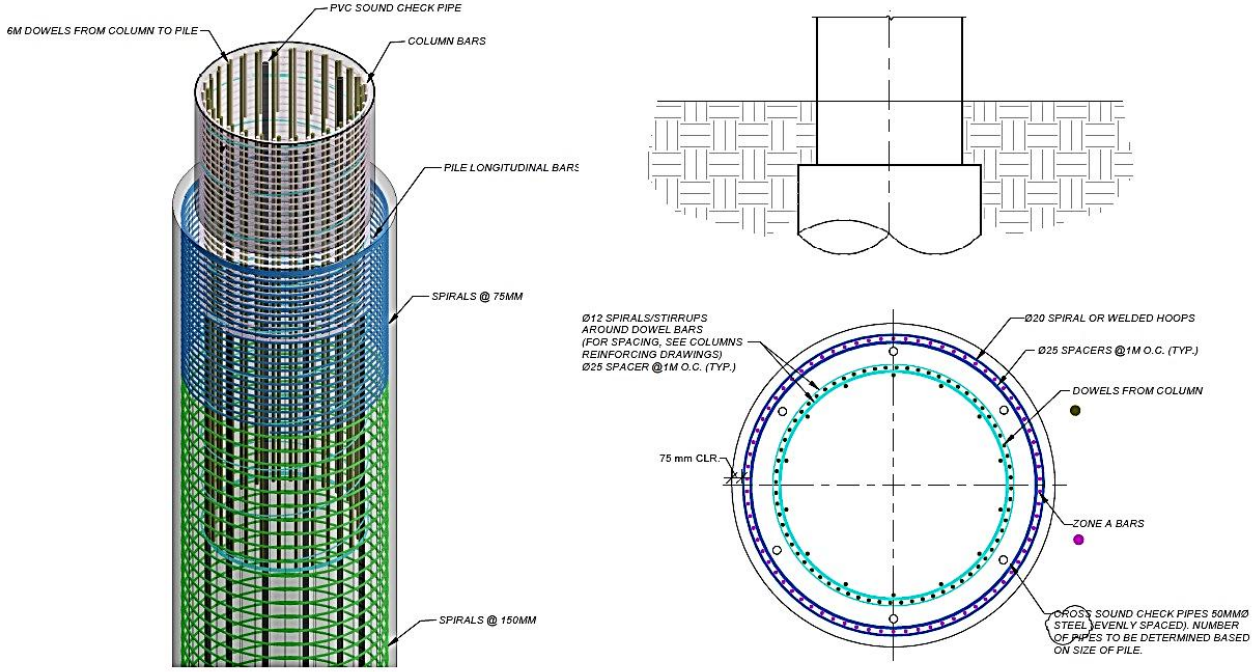

Fig. 2 The detail of the monopile of the Monorail and the column connection (Nile Office for Engineering Consulting Innova Transportation, 2020)

2.1 Loading Technique and Results

In-situ test of both standard penetration test and pressure-meter test are carried out to estimate SPT-N and elastic modulus (E_S) respectively. Table 4 shows the soil profiles and results of both In-situ and lab tests. A detailed geotechnical investigation was carried out prior to monopiles construction, which out-lined the underlying soil formations around the selected monopile with the various strati-graphic units, as illustrated in Fig. 3.

The loading tests are carried out in two cycles of loading and unloading, which the loading of 1st cycle is up to design load followed by gradually removing the loads, then the 2nd cycle of loading up to maximum load as shown in Table 5. The experimental process is conducting for the non-working pile by applying anticipated static load as detected in Fig. 4.

The measurements of settlement of piles recorded during to loading cycles. However, the maximum settlement for pile No.1 is 7.01 mm at load equal 12.47 MN as detected in Fig. 5.

Table 4 Description and properties of soil layers (Mossallamy consulting office, 2020)

Pile No.	Soil description	Depth (m)	SPT-N	γ kN/m³	G_S	W_C %	E_s MN/m²	Gravel %	Sand %	Fine %	C kN/m²	φ degree
01	Fill	0.50		18.00								29
	Medium dense Sand	1.50		22.60			37					38
	Grey silty Clay and silty Sand	1.05		20.00			60				11	34
	Medium to very dense yellow fine to coarse Sand	4.60	45	22.90		4.9	60					42
		10.95	48		2.62	2.3	60	0.00	88.00	12.00		
		30.10	>50		2.66		60	0.00	97.00	3.00	16	

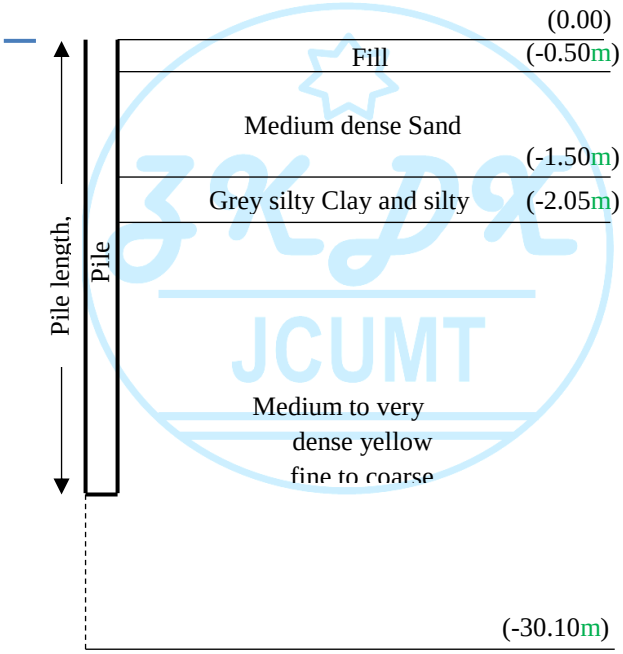

Fig. 3 Subsurface ground conditions around monopiles, (Consulting Bureau Prof. Adel Gabr, 2020)

Table 5 the sequence of loading during pile loading test. (Consulting Bureau Prof. Adel Gabr, 2020)

Cycle	Total Time	Total Load	Average Settlement
No. 1	15.00	100.00	0.30
	30.00	200.00	0.63
	45.00	300.00	1.04
	60.00	400.00	1.41
	120.00	**500.00**	1.84
	130.00	300.00	1.11
	140.00	50.00	0.44
	141.00	0.00	0.29
No. 2	157.00	50.00	0.40
	172.00	200.00	0.81
	187.00	300.00	1.15
	202.00	400.00	1.54
	262.00	500.00	1.94
	277.00	750.00	2.74
	292.00	1000.00	4.06

	1012.00	**1250.00**	7.01
	1022.00	1000.00	6.66
	1032.00	500.00	5.40
	1042.00	250.00	4.58
	1052.00	0.00	3.54

Fig. 4 Field photo of axial static load test, (The Arab Contractors, Foundation department, 2020)

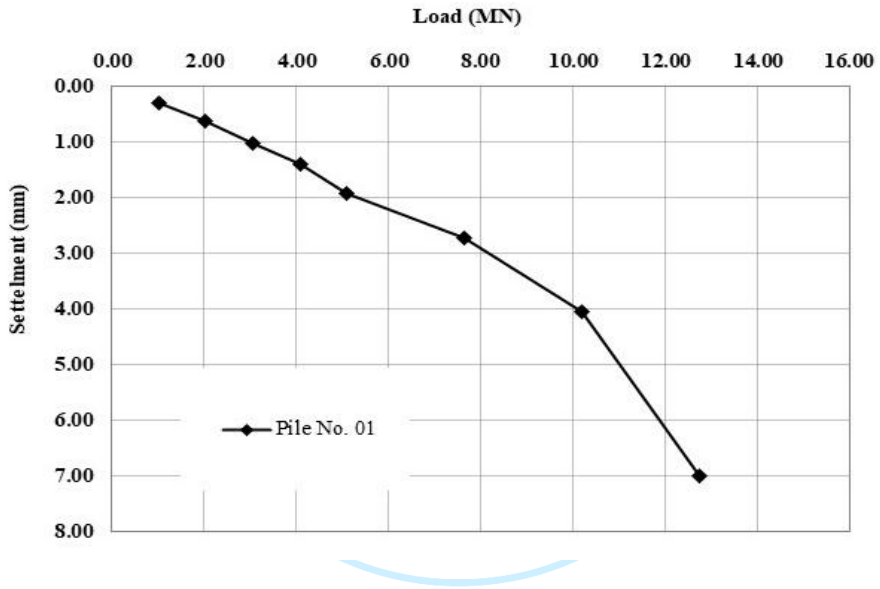

Fig. 5 Load-settlement curve of vertical loading test, (Consulting Bureau Prof. Adel Gabr, 2020)

3. Numerical Analysis

A finite element numerical model is developed to study large-diameter monopiles, the effect of vertical loading and pile length on both shaft resistance and tip resistance. To achieve the aim of this research, the PLAXIS 3D V20 program is used. The finite element simulation is carried out for pile No.1, and the soil parameters are determined from soil investigation data as shown in Table 4. A hardening soil material is used, and the drainage type is considered. An elastic behavior of embedded beam and linear axial skin resistance are used to simulate the monopile, and the pile properties are listed in Table 6. The skin resistance at the top and the end of the embedded beam are 200 kN/m and 500 kN/m respectively.

Table 6 Property of embedded beam – pile

Pile property	Unit	Value
Es	kN/m^2	30.00E6
Diameter (D)	m	2.00
Length (Lp)	m	18.00
γ	kN/m^3	24.00

The element of soil mass is 10-noded. The plan dimensions is (60 x 60) m which is about (30D). The negative Z-direction is $4*L_p$ as shown in Fig. 6. The model boundary conditions are determined after conducting preliminary sensitivity analyses concerning its effect on the pile vertical displacements [2]. Also, it is seen that the four surfaces displacement around soil mass are hinged displacement in both directions X and Y, and free displacement in Z direction. The base of model is fixed displacement in Z direction.

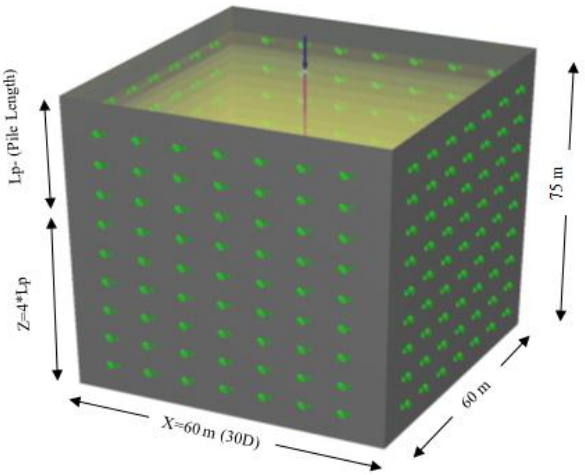

Fig. 6 The soil mass and pile structure

3.1 Model verification

A loading test arrangement was applied to simulate the full-scale vertical loads value. Fig. 7 shows the calculated displacement around the pile at the final stage of loading.

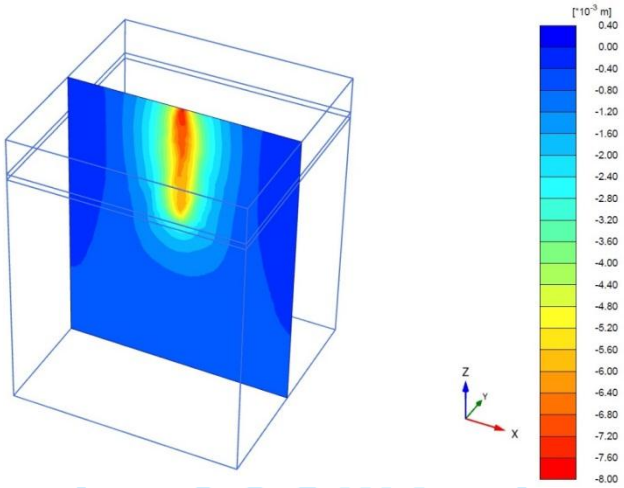

Fig. 7 The total displacement at vertical load equal 12.47 MN.

Fig. 8 shows a comparison between measured and estimated data. The results of the study indicate that there is a good agreement between the calculated and measured data. During the loading cycle, the maximum settlement was calculated to be 7.50 mm, which is 7% higher than the in situ maximum settlement. However, during the unloading stage, the difference between the measured and calculated data was 26%.

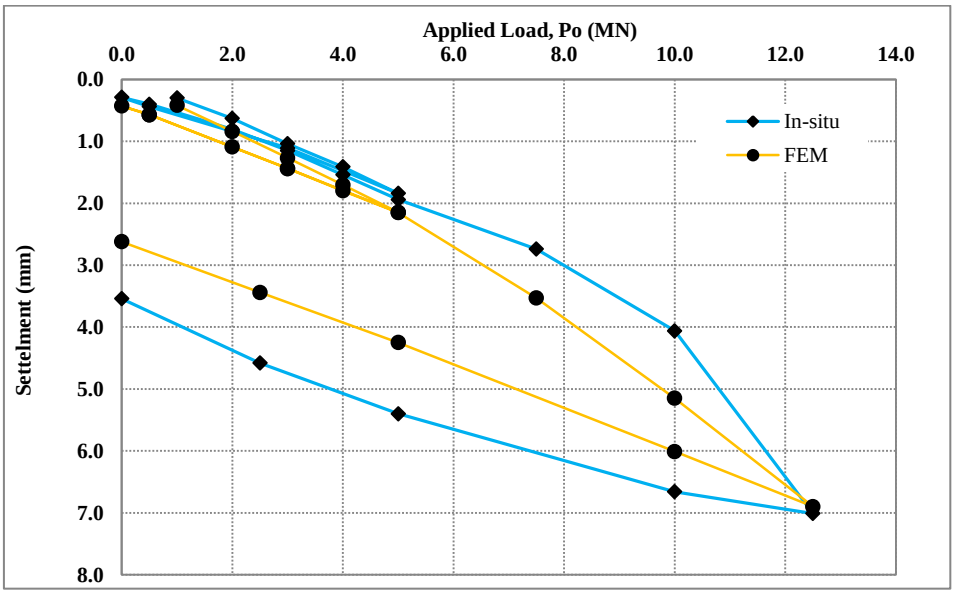

Fig. 8 The load-settlement curves.

3.2 Parametric Studies

A series of parametric studies was carried out to investigate the optimum pile length and its effect on pile capacity. The analyses were done with eight pile lengths starting from 14 m up to 30 m. The model configuration used in parametric studies was as that conducting in verification case. Also, the soil type in the last layer was assumed to be extended up to 4 times the pile length.

The load-settlement curve for the eight-analysis done on monopile with changing the pile length in each case. The test load is adopted to be 40 MN ($8*Q_d$) instead of 12.5 MN. The primary goal of increasing the pile load test is to determine the safe capacity of a tested pile and to verify the design calculations computed by traditional methods. All loading-settlement curves for all cases of pile length do not reach the ultimate load at settlement of the 10% of pile diameter as detected in Fig. 9. Moreover, the increase in pile length leads to decrease settlement and hence increase its capacity which can be seen clearly in case of L_P30.

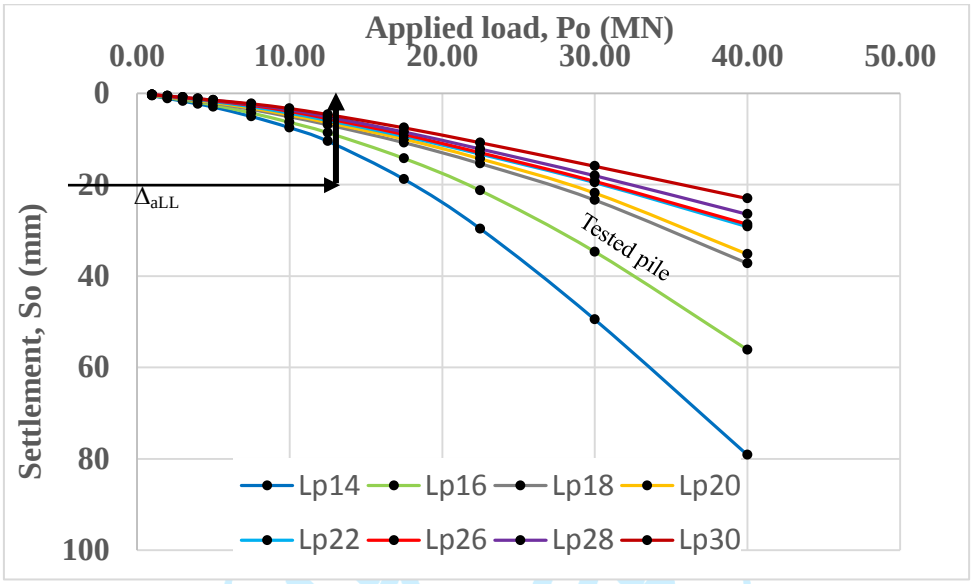

Fig. 9 The load-settlement curves

The logarithmic load versus the settlement is plotted in **Fig. 10.** The relation is linearly up to 5 MN for all pile lengths. Hence, the design load (Q_d) is the same as the yield load (F_y) which is un dependent on the pile length.

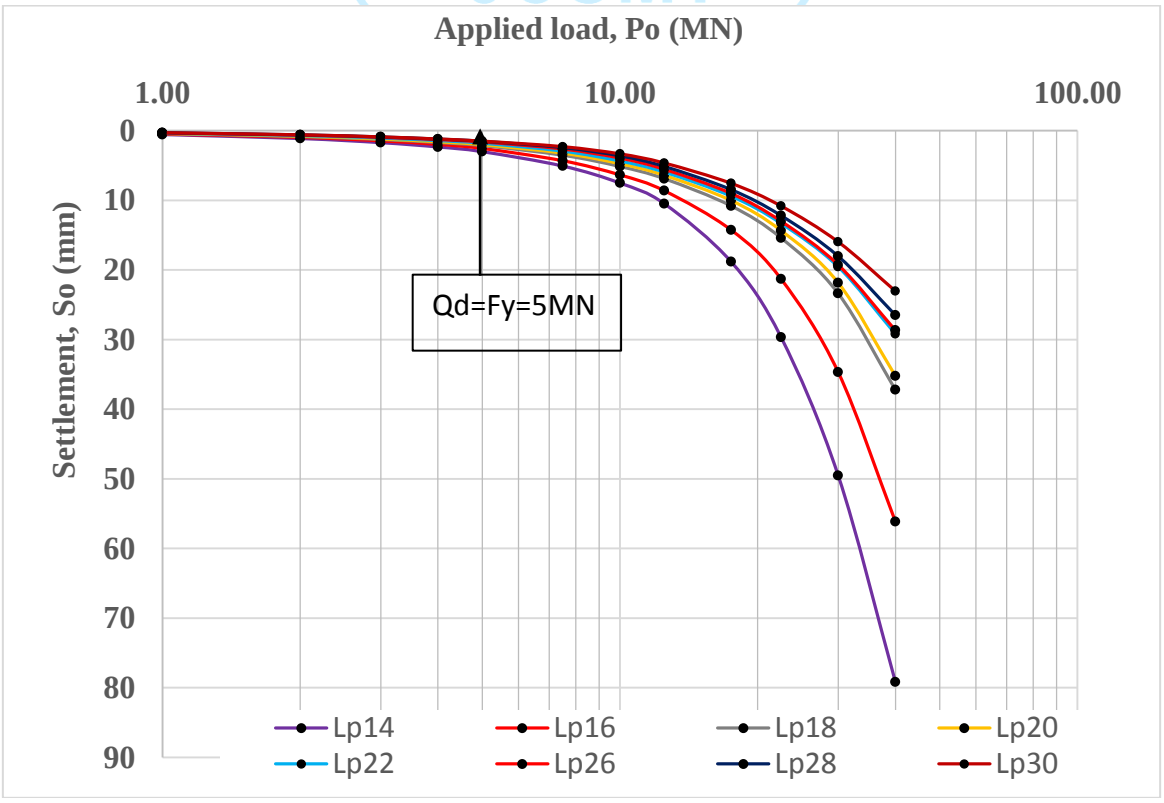

Fig. 10 Semi-logarithmic of the pile load-settlement curves.

3.3 Prediction of ultimate pile capacity from Chin method under different test loads

The Modified Chin method is the commonly method used to determinate the pile capacity from load-settlement curve. The settlements values are divided by their associated load are plotted against the settlement as elaborated in Figs. 11&12. The ultimate pile capacity is determined by considering two applied loads. The first load is 1.5 times the design load (7.5MN). The second load is equal to 8 times the value of Qs (40 MN) as detected in the Table 7. It is evident that there is a discrepancy between the ultimate capacities estimated using test loads of 7.5 MN and 40 MN. This difference is particularly noticeable when L/D is less than 10 or greater than 13. Consequently, an alternative method is required to validate the limitations of the Chin method.

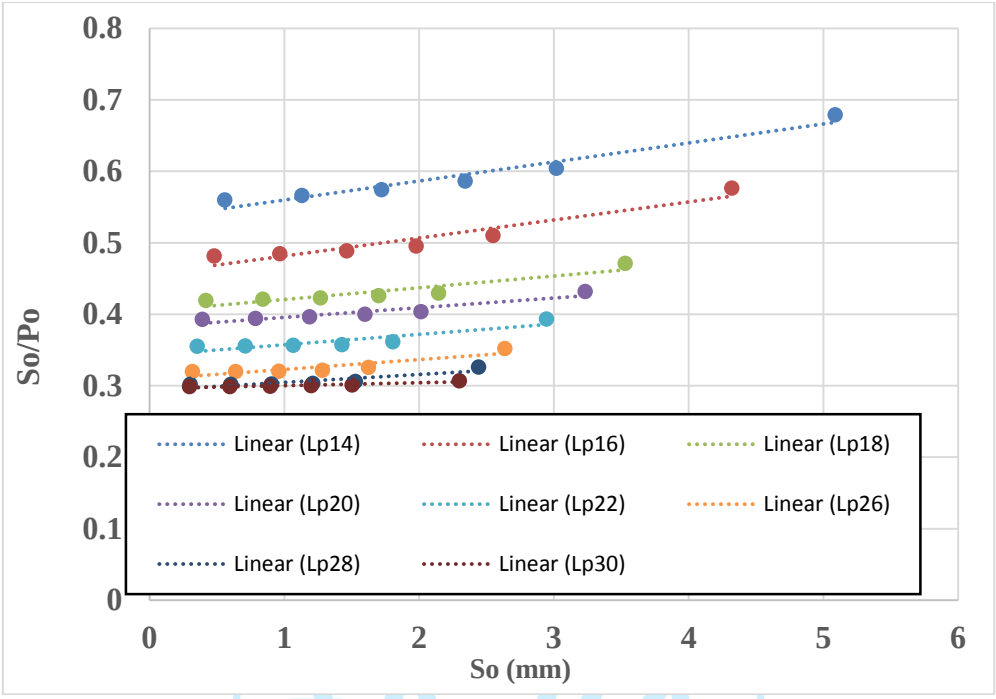

Fig. 11 Chin method for test loading up to 7.5 MN

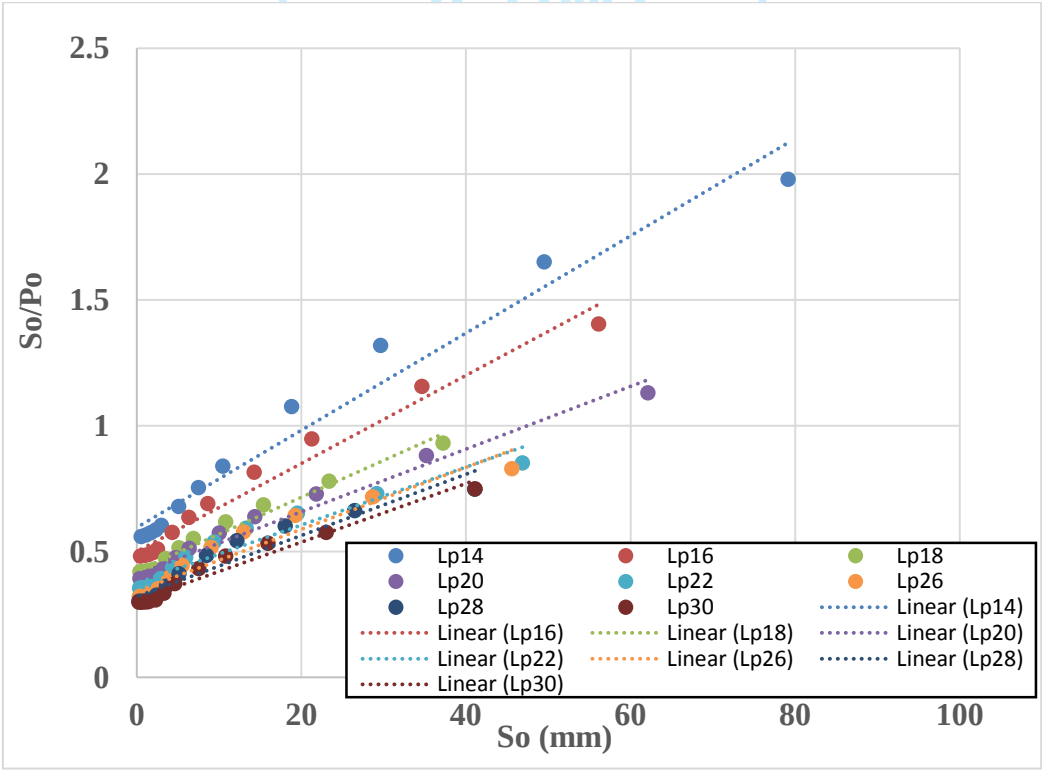

Fig. 12 Chin method for test loading up to 40 MN

Table 7 Pile length and ultimate capacity up to 40 MN of axial loading (Modified Chin)

Pile length, L_P (m)	Pile diameter, D (m)	Test load 7.5MN		Test load 40MN		$\frac{(Qu1-Qu2)}{Qu2}$*100
		Slop of line, b	Ultimate load, Q_{u1} (MN) $Q_u = 1/1.2b$	Slop of line, b	Ultimate load, Q_{u2} (MN) $Q_u = 1/1.2b$	
14	2	0.0266	31.3	0.0193	43.2	27.8%
16	2	0.0251	33.2	0.0175	47.6	30.3%
18	2	0.0164	50.8	0.0155	53.8	5.6%
20	2	0.0135	61.7	0.0147	56.7	8.8%
22	2	0.0145	57.5	0.0143	58.3	1.4%
26	2	0.0139	60.0	0.0156	53.4	12.4%
28	2	0.011	75.8	0.0155	53.8	40.9%
30	2	0.004	208.3	0.0139	60.0	246.7%

3.4 Prediction of Ultimate Pile Capacity from Chin Method under Different Test Loads

Comparatively, the pile is more complex to estimate its ultimate capacity and has a greater impact on the economy of a project. ECP method with unique assumptions and limitations are available to interpret ultimate pile capacity based on the results of the pile load test. Elsamny et al. (2017) reported that the ECP method is in a good agreement with pile load test interpretation method conducted on single pile in cohesionless soil. Therefore, this study provides a quantitative analysis of Chin and ECP method and investigates the most suitable and reliable interpretation method to be adopted for cast in situ piles. The maximum acceptable settlement of pile can be calculated using equation (4) according to the Egyptian code of soil Mechanics and foundation design,

$$S_Q = 0.02D + 0.5QL/AE \quad (4)$$

Where D is pile diameter, Q is 2.5 times of design load, L is pile length, A is pile section area, and E is elastic modulus of pile material.

To apply equation (4), the pile is needed to be loaded to reasonable value cause settlement more than the ultimate settlement. The ultimate pile load can be estimated from the maximum acceptable settlement, as shown in Fig. 13 and Table 8.

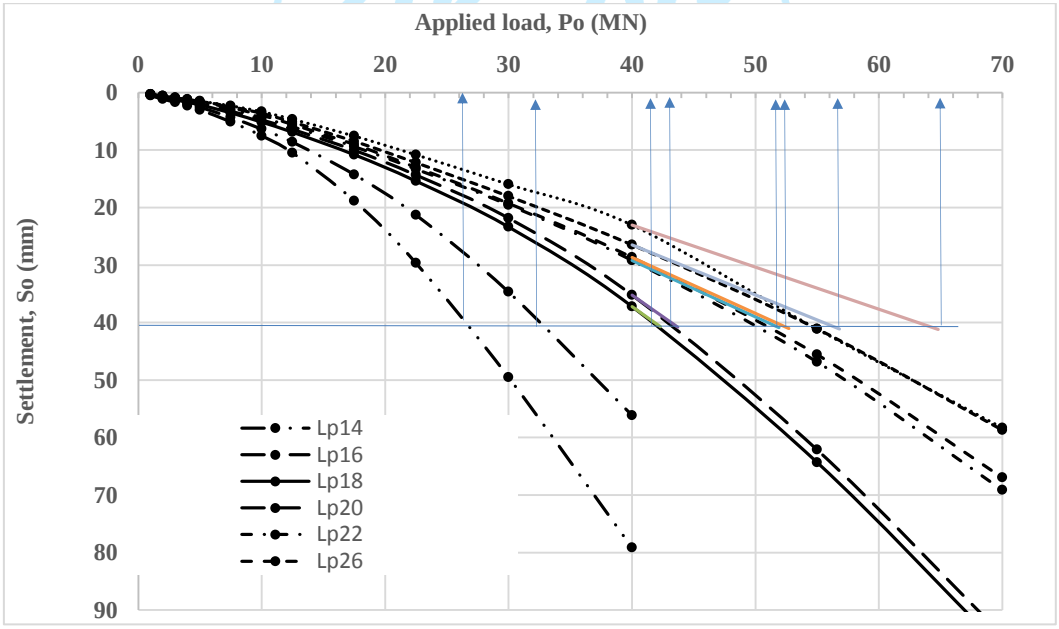

Fig. 13 Pile ultimate capacities from Equation 4 (ECP)

Table 8 Pile length and ultimate capacity (ECP)

Pile length, L_P (m)	Pile diameter, D (m)	Sett., S_Q (mm)	Ultimate load, Q_u (MN)
14	2	40.56	26.3
16	2	40.64	33.2
18	2	40.72	42.1
20	2	40.80	43.9
22	2	40.88	50.1
26	2	41.04	50.2
28	2	41.11	55.0
30	2	41.19	55.1

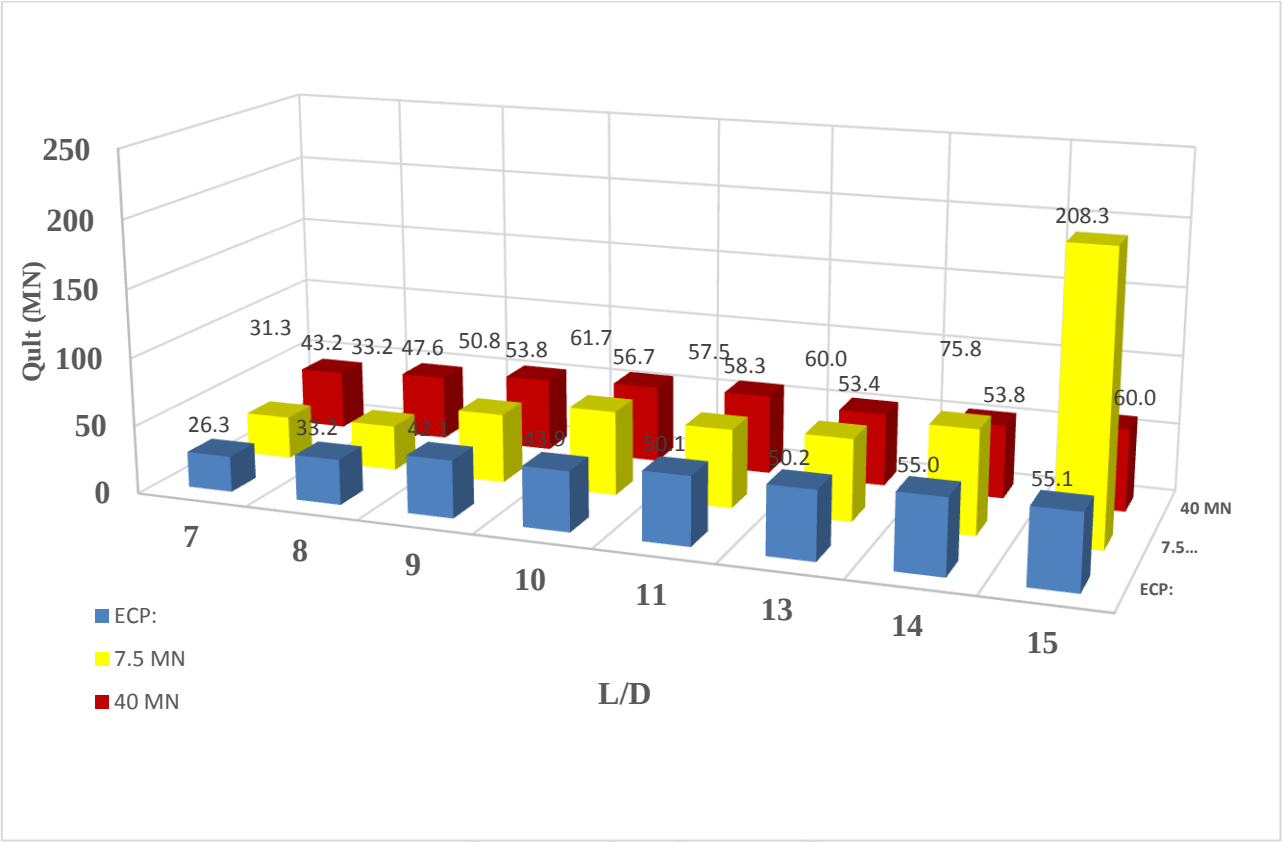

Fig. 14 Comparison between pile ultimate capacities form ECP and Chin methods

It is observed from Fig. 14, the comparison between pile ultimate capacities form ECP and Chin methods in which the pile lengths were normalized to pile diameter. It is noticed that the ultimate pile loads calculated using the Chin method are greater than that calculated using the ECP. Marcos et al. (2013) documented the same result.

The Chin method is a dynamic test used to determine the capacity of a pile. According to a comparative study of various interpretative methods of the pile load test, the maximum difference is ranging between 40% to 278% which is observed when the testing load is 1.5 times the design load and L/D≥13. If the testing load adopted in chin method is equal to 8 times the design load (8*Qd) and L/D<10, the ultimate capacity of the pile will be greater than both the ECP method and the Chin method under testing load $1.5Q_d$ by about 40% to 60%.

To summarize, the Chin method's accuracy is dependent on the pile length and testing load. If the ratio of pile length to pile diameter is greater than or equal 13, the pile testing load can be increased up to $8Q_d$ to obtain a reliable result using the Chin method. Additionally, the accuracy of the pile load test of pile length ratio (L/D<10) increases by applying testing load up to $1.5Q_d$. Moreover, for pile length to pile diameter ratio between 9 to 11, the ultimate capacity of the pile using the Chin method is independent of the pile applied load and there is a good agreement with that estimated by ECP method.

Generally, the two mentioned method either ECP or Chin method was considered by taking the average of their results.

3.2.1 Shaft Resistance Estimation

As for the theoretical equation, the ultimate load can be expressed as the summation of the ultimate shaft load and tip load. Curves in Fig. 15 show the axial force in L_P18 at 12 cases of loading from 1 MN to 40 MN. To estimate the shaft resistance, one can use the difference between the axial load values at the top and tip of the pile, which is known as the friction load (Qs) [15].

Fig. 16 displays the shaft load (Q_s) for the eight cases of pile length with normalization of pile settlement. Likewise, the unit shaft resistance reaches the peak value at 15% of ultimate pile load which calculated from ECP. Furthermore, for any length of pile, the shaft resistance is fully mobilized at the settlement value=0.5% times the pile diameter. After that, the shaft resistance remains constant. Additionally, the unit shaft resistance (q_s) is equal to 45 kN/m^2 for all cases. Then the shaft resistance can be estimated as follows.

$$q_s = 45\,\pi\,D\,L\ \ (kN) \qquad (5)$$

Which D and L are the pile diameter and embedded length respectively.

Moreover, the percentage of load transferred to surrounding soil at yield load of pile (Fy=5MN) is ranging between 6.6% to 10% of applied load as shown in Fig. 17.

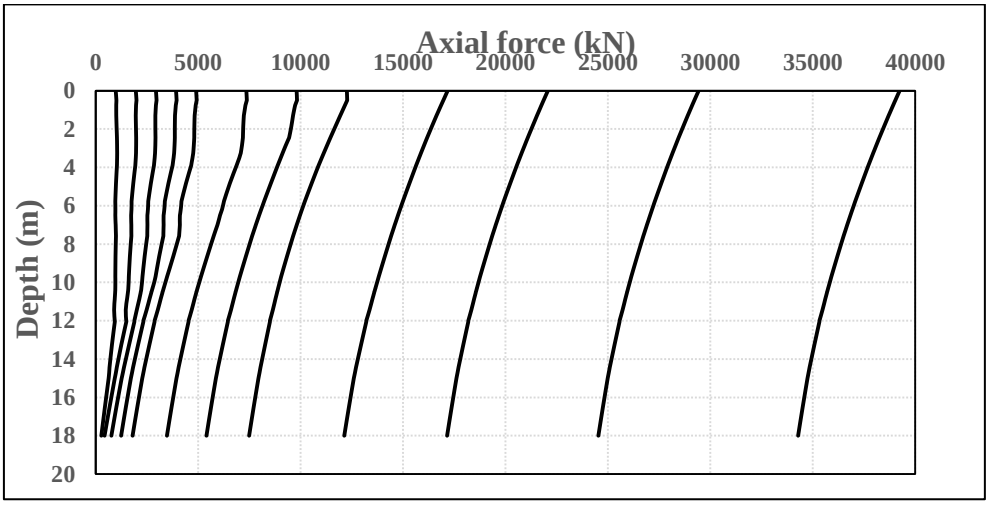

Fig. 15 Axial force distributions of pile L_P18 according to different loads

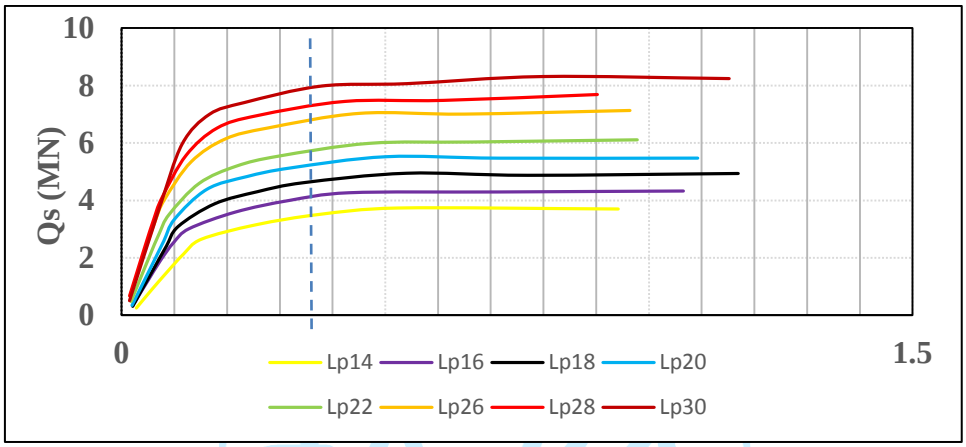

Fig. 16 Variations of shaft load (Q_s) for the eight cases of pile length and normalization of pile settlement

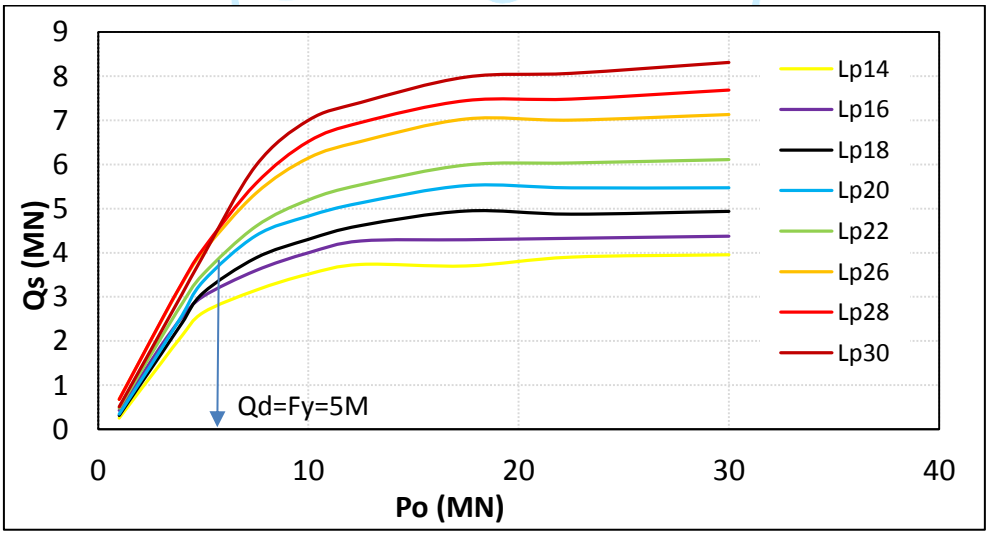

Fig. 17 Variations of shaft load (Q_s) for the eight cases of pile length with the applied load

Fig. 18 shows the logarithmic relationship between the shaft load (Q_s) and the normalizati on of pile settlement (S_o/D). It is observed from Fig. 17 that the shaft load increase linearly up to the yield load at 0.35 S_o/D, then the relationship deviates to be constant up to ultimate shaft load at 0.5% S_o/D. This likely suggests that the value of Q_{sy} depends on the pile length which increases with increasing the pile length. Generally, the shaft load can be estimated by the following equation.

$$\boldsymbol{Qs = (0.2775L - 0.017)\, In\, \frac{S_0}{D} + 0.37L - 0.56} \qquad (6)$$

Which *Qs* is shaft load for S_o/D < 0.35, yield shaft load (Q_{sy}) for S_o/D = 0.35, and ultimate shaft load (Q_{su}) for S_o/D = 0.5. The accuracy of equation (6) can be demonstrated by comparing its results with that estimated from Fig 15. It can be observed that there is a good agreement between the two results as shown in Fig. 19.

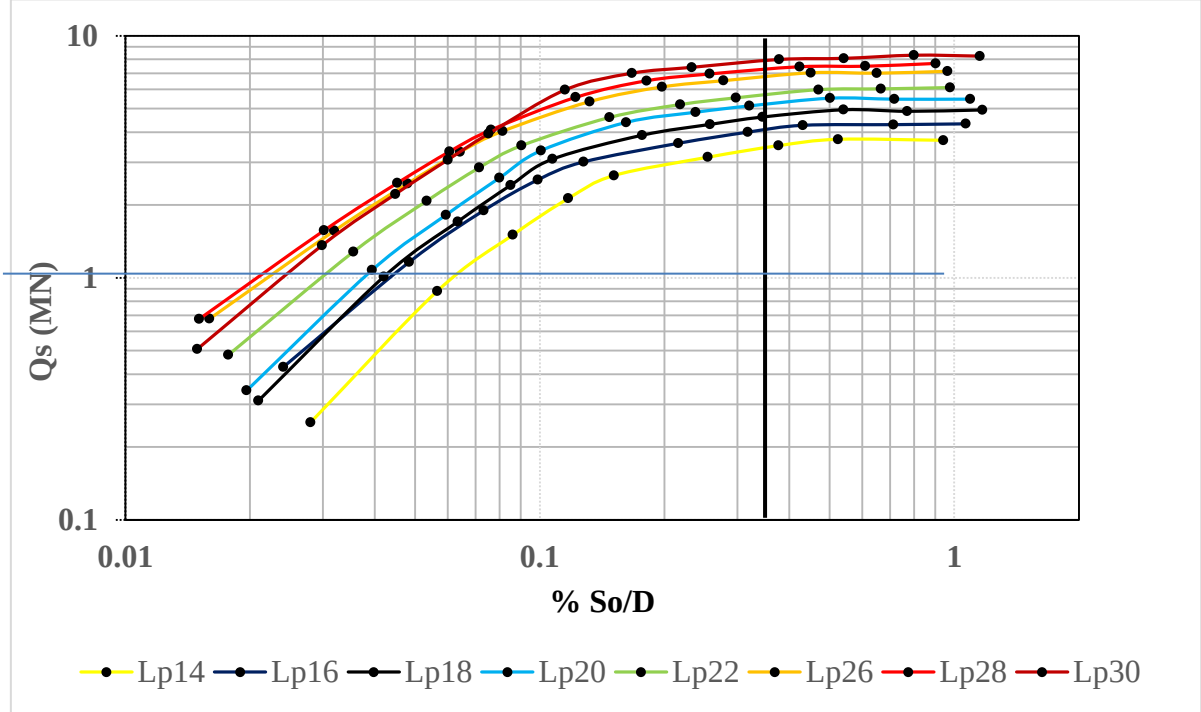

Fig. 18 logarithmic relationship between the shaft load (q_s) and the normalization of pile settlement.

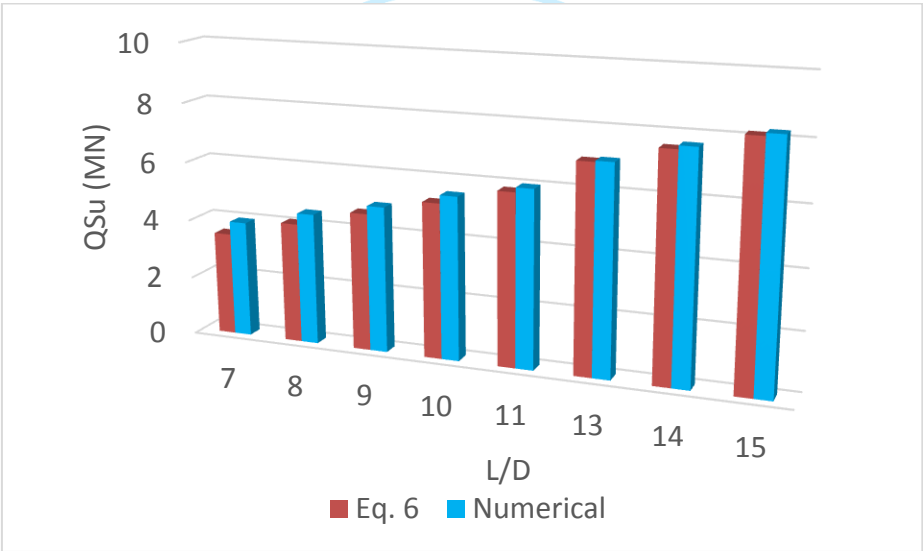

Fig. 19 comparison between the shaft resistance estimated from numerical and equation (6)

3.2.2 Tip Resistance Estimation

The applied load on pile is the sum of the shaft load (Q_s) and the base load (Q_b). Accordingly, the tip resistance can be expressed by the difference between applied load and friction load. The percentage of load transmitted to the tip can be expressed by the ratio (γ) as shown in equation (7)[15].

$$\gamma = \frac{P_o - Q_s}{P_o} * 100\ (\%) \qquad (7)$$

Which P_o is the applied load and Q_s the shaft load.

Fig. 20 illustrate the variations of the tip resistance (Q_b) with the load transmission ratio (γ). In general, when a pile is loaded, the load is initially distributed between the shaft and the tip of the pile. As the load increases, the pile tip bears most of the load, with the load transmission ratio γ covering between 80% and 90% of the applied load. However, as the pile length increases, the pile tip resistance decreases. Therefore, increasing the pile length is considered an appropriate solution for high compressible bearing layers. Furthermore, the bearing load at the pile yield load or the working load (F_y=5MN) ranges between 2.5% to 7.5% of applied load according to pile length. Fundamental to note that, the total applied load was predominantly carried by friction at the working load, as percentage of the transferred load by friction at this stage ranges between 6.6% to 10% of the total applied load.

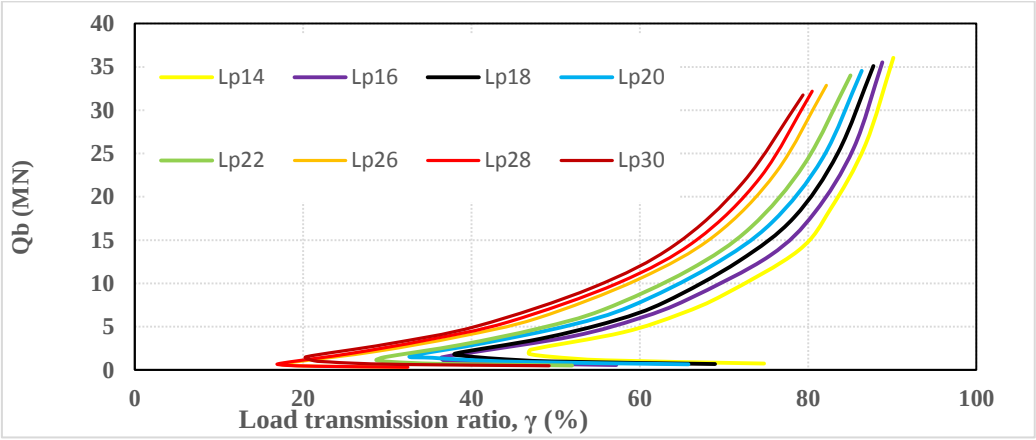

Fig. 20 Relationship between the unit tip resistance and the load transmission ratio

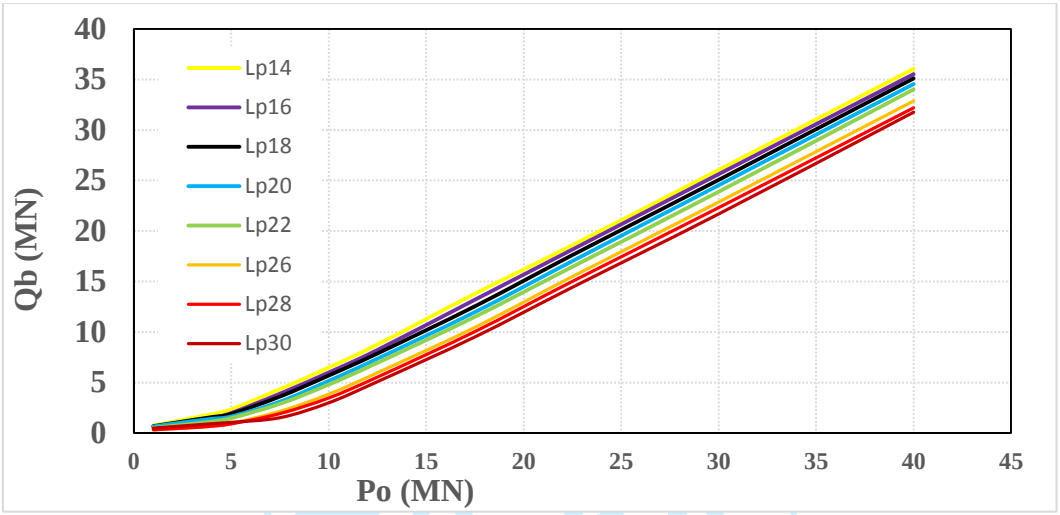

Fig. 21 The relation between the bearing load and applied load with respect to (L/D)

Fig. 22 displays the tip load (Q_b) for the eight cases of pile length with normalization of pile settlement. The percentage of transferred load by bearing was very small at the initial loading increments, then increased to be about 88% of the total applied load at the of ($8Q_d$). Also, the maximum bearing load for pile length to pile diameter ratio ($L/D \geq 9$) is achieved at settlement does not exceed 2% of pile diameter (D). However, for pile length to pile diameter ratio ($L/D < 9$), the maximum bearing load is demonstrated at settlement ranges from 3% to 4% of the pile diameter (D).

Moreover, Fig. 23 elaborates the relation between the bearing load, shaft load and the ratio of pile length to its diameter (L/D). The tip load transferred to bearing soil decreases with increasing the pile length due to decreasing the pile settlement and vice versa in case of shaft resistance.

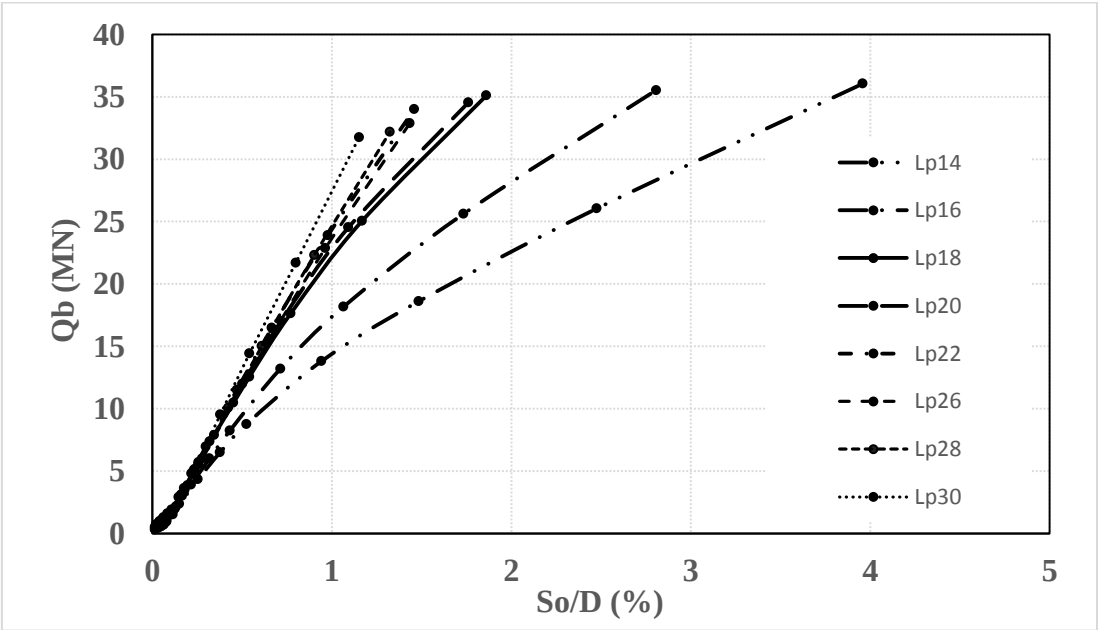

Fig. 22 Variations of tip load (Q_b) for the eight cases of pile length and normalization of pile settlement

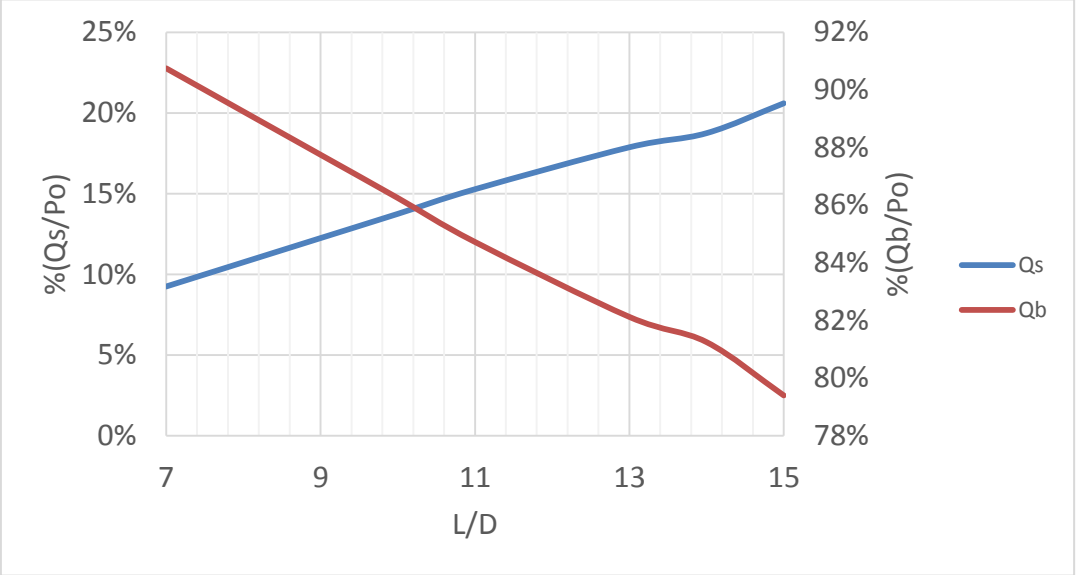

Fig. 23 The variation of percentage of friction and bearing load to applied load with respect to (L/D)

4. Conclusions

Full-scale vertical loading test was performed for a large diameter bored piles in sandy soil at the Cairo Monorail project. 3D numerical model using Plaxis software was created to investigate its capabilities to simulate the pile loading test. There is good matching between the load–displacement relation attained through field test and that estimated by numerical model.

A series of parametric studies was conducted on the same model used in the verification case. The analyses were with altering pile length. The applied test load is adopted to be 40MN instead of 12.5MN. From the results of these analyses, it can be deduced the followings.

1) Despite the applied load being eight times greater than the design load, the necessary displacement (10% D) to reach the ultimate load is not attained. This could be due to the exceptional stiffness of the bearing layer.
2) The design load (Q_d) is the same as the yield load (F_y) which is un dependent on the pile length and equal to 5MN.

The Chin method, which involves applying two distinct loads, is used to estimate the ultimate pile capacity in relation to pile length. Additionally, the Egyptian code of practice equation (ECP) serves as an alternative approach to verify the reliability of the Chin method. The outcomes from comparing these two methods can be summarized as follows.

1) The ultimate pile capacity, as determined by the Chin method, appears to be overestimated when its results are compared to those calculated using the ECP method.
2) The Chin method appears suitable if the applied load is eight times the design load, and the ratio of the normalized pile length to its diameter (L/D) is greater than or equal to 13. Conversely, for a short pile where L/D is less than 10, the Chin method remains reliable when conducting an axial load approximately 1.5 times the design load.
3) The ECP method, which considers both the pile length and the applied load, is deemed more conservative in its computation of the ultimate capacity, despite these factors. Accordingly, the values of two pile ultimate capacity calculated by two stated methods are considered by taking the average of their results.

Estimating the ultimate pile capacity is a complex issue with significant economic implications for projects. As such, numerical calculations were performed on the shaft and bearing loads to derive a specific relationship or formula. This formula is intended to calculate the ultimate capacity, which is the sum of these two values, offering an alternative to the theoretical equation provided by the Egyptian code. The following can be deduced from numerical analysis.

1) The shaft resistance is fully mobilized at a settlement value equals 0.5% of pile diameter and equal to 45 kN/m^2 for all cases of pile length. The peak value of shaft resistance at 15% of ultimate pile load is calculated from ECP.
2) The applied load is distributed between the shaft and tip at the beginning of loading. The major load is transmitted to tip resistance. This tip resistance increases gradually and reaches its peak value to be from 80% to 90% of the applied load.
3) The beak value of tip resistance is achieved at settlement value not exceeded 2% of pile diameter (D) for $L/D \geq 9$. Also, for $L/D < 9$, the maximum bearing load is demonstrated at settlement ranges from 3% to 4% of the pile diameter (D).
4) The relationship between the shaft load (Q_s) and the normalized pile settlement (S_o/D) can be described logarithmically. This relationship demonstrates that the shaft load increases in a linear fashion until it reaches the yield load at 0.35 S_o/D. Beyond this point, the relationship plateaus and remains constant until it reaches the ultimate shaft load at 0.5% S_o/D. This pattern suggests that the shaft load value can be estimated using an equation that takes into account both the pile length and the normalized settlement.

5) The bearing load, when at the pile yield load or working load (F_y = 5 MN), varies from 2.5% to 7.5% of the applied load, depending on the length of the pile. It's crucial to understand that the majority of the total applied load is borne by friction at the working load. Specifically, the fraction of the load transferred by friction at this stage is between 6.6% and 10% of the total applied load.

Acknowledgements
The authors thank the Arab Contractors Company - Foundation Department for allowing to attend the in-situ loading tests.

Author Contributions
Baset M. A: Modeling, writing - original draft; El-Attar A. N.: Conceptualization, Investigation, Methodology writing; Bahr M. A., &Hassan A. A.: Review & editing.

Funding
The authors have no relevant financial or non-financial interests to disclose.

Competing Interests
The authors have no competing interests to declare that are relevant to the content of this article.

References
1. Ahmed Majeed et. al. (2018). Simulation of bearing capacity of bored piles. MATEC Web of Conferences 162, 01004.
2. Daniel K. T. (2019). Numerical Simulation of Static Pile Load Test on Stratified Soil Deposits. Partial Fulfillment for the Degree of Master of Science, Addis Ababa University.
3. ECP 202/4. (2005). Egyptian code for soil mechanics – design and construction of foundations. Part 4, Deep foundations.
4. Eurocode 7: Geotechnical Design section 7.
5. F. K. Chin (1970). Estimation of the ultimate load of piles from tests not carried to failure. Proc., 2nd. South-East Asian Conf. on Soil Eng., Singapore.
6. H. Meibner, H. Shen and W. F. Van Impe (1993). Punching effects for bored piles. Conference on Deep Foundations and Auger Piles, Rotterdam.
7. Hyeong et. al. (2007). Analysis of Static Axial Load Capacity of Single Piles and Large Diameter Shafts using Nonlinear Load Transfer Curves. KSCE Journal of Civil Engineering Vol. 11, No.6.
8. M. Eid et. al. (2018). Numerical Analysis of Large Diameter Bored Pile Installed in Multi Layered Soil: A Case Study of Damietta Port New Grain Silos Project. International Journal of Current Engineering and Technology.
9. M. Ezzat et. al. (2019). Numerical Simulation of Axially Loaded to Failure Large Diameter Bored Pile. World Academy of Science, Engineering and Technology International Journal of Geotechnical and Geological Engineering Vol:13, No:5, 2019.
10. PLAXIS 3D Reference Manual Edition 20.04 (2020).
11. Standard Test Methods for Deep Foundations under Static Axial Compressive Load ASTM - D1143.
12. Tarek N. Salem et. al. (2020). Modeling of Large Diameter Piles in Soil Formations Including Soft Clay. PORT-SAID ENGINEERING RESEARCH JOURNAL Faculty of Engineering - Port Said University Volume 24 No. 1 March 2020 pp: 44:53.
13. Terzaghi, K. (1943). Theoretical Soil Mechanics. John Wiley & Sons Ltd., 510.
14. Weibull, W. (1951). "A statistical distribution function of wide applicability." J. App. Mech., 18(3), 293–297.
15. W. F. VAN IMPE (1993). Deep Foundations on Bored and Auger Piles. 2nd International Geotechnical Seminar on Deep Foundations on Bored and Auger Piles, Belgiun., 1993.
16. Nile Office for Engineering Consulting Innova Transportation, (2020) "structural engineering report: Cairo Monorails new Administrative Capital and 6th of October lines Egypt"
17. Consulting Bureau Prof. Adel Gabr, (2020), "pile load test report: Cairo Monorails new Administrative Capital and 6th of October lines Egypt."
18. Mossallamy consulting office, (2020), "Geotechnical Investigation Report: Cairo Monorails new Administrative Capital and 6th of October lines Egypt."
19. The Arab Contractors, Foundation department, (2020) "Main contractor of Cairo Monorails new Administrative Capital and 6th of October lines Egypt."
20. Elsamny M, Ibrahim MA, Gad S, Abd-Mageed M (2017) Experimental evaluation of bearing capacity and behavior of single pile and pile group in cohesionless soil. Int J Eng Res Technol 6:695–704
21. Marcos MCM, Chen YJ, Kulhawy FH (2013) Evaluation of compression load test interpretation criteria for driven precast concrete pile capacity. KSCE J Civ Eng 17:1008–1022.